

# Study on the Dimensional Changes and Residual Stresses in Carbonitrided and Ferritic Nitrocarburized SAE 1010 Plain Carbon Steel

Chunyan Nan<sup>1,a</sup>, Derek O. Northwood<sup>1,b</sup>,

Randy J. Bowers<sup>1,c</sup> and Xichen Sun<sup>2,d</sup>

<sup>1</sup>Department of Mechanical, Automotive and Materials Engineering

University of Windsor, 401 Sunset Ave., Windsor, Ontario, Canada N9B 3P4

<sup>2</sup>Chrysler LLC, Auburn Hills, Michigan, U.S.A.

<sup>a</sup>nan@uwindsor.ca, <sup>b</sup>dnorthwo@uwindsor.ca, <sup>c</sup>rbowers@uwindsor.ca, <sup>d</sup>js154@chrysler.com

**Keywords:** carbonitriding, ferritic nitrocarburizing, dimensional distortion, residual stress.

**Abstract.** Carbonitriding is a metallurgical surface modification technique that is widely used in the automotive industry to increase surface hardness and wear resistance. Given the problems associated with carbonitriding, such as dimensional distortion, oxidation and non-uniform surface hardness, nitrocarburizing has been proposed as an alternative heat treatment method to improve the surface characteristics. The major advantages of ferritic nitrocarburizing are the minimal dimensional changes and distortion due to the low process temperature at which no phase transformations occur. This increases productivity and product quality, and decreases costs.

The focus of this study was to determine the effects of carbonitriding and ferritic nitrocarburizing processes on the dimensional changes and residual stresses in a steel used for automotive applications. Navy C-ring specimens and prototype stamped parts made from SAE 1010 plain carbon steel were used in the testing. Gas, vacuum and ion ferritic nitrocarburizing processes with different heat treatment parameters were investigated. X-ray diffraction techniques were used for the residual stresses evaluation and surface phase analysis of the specimens.

## Introduction

The surface properties of ferrous metals can be greatly improved by thermochemical diffusion processes which introduce carbon and nitrogen into the alloy. Carbonitriding is a widely accepted case-hardening process used by the automotive industry. It is usually carried out at temperatures ranging between 705 and 900 °C and produces a carbonitrided case between 0.075 to 0.75 mm [1-3]. During the carbonitriding process, the austenite composition is changed and high surface hardness is obtained by quenching to form martensite. However, the phase transformation to martensite upon quenching results in dimensional changes [2, 3]. Moreover, surface oxidation takes place during the processing, and non-uniform surface hardness occurs due to the delayed heat transfer between the quenching die and the work part.

Nitrocarburizing as another form of surface hardening that has been a proven process for many years. Nitrocarburizing is also referred to as ferritic nitrocarburizing because the nitrogen and carbon are introduced to the surface of ferrous materials at temperatures completely within the ferrite phase field [4]. The ferritic nitrocarburizing temperature ranges between 525 and 650 °C [5], and produces a very thin compound layer with a thickness between 10 and 40 µm [4]. The compound layer, which is composed of single-phase epsilon (ε) iron-carbonitride (Fe<sub>2-3</sub>(N,C)), has excellent wear and antiscuffing properties. Beneath the compound layer is the diffusion zone, which consists of gamma prime (γ') and ε phase, cementite, and various alloy carbides and nitrides [4, 6]. One major advantage of ferritic nitrocarburizing is the smaller dimensional distortion due to the low temperature process and the absence of phase transformation from austenite to martensite [5]. Because quenching is not a necessary process for ferritic nitrocarburizing, the surface oxidation and non-uniform surface hardness associated with quenching can be significantly reduced.

Different ferritic nitrocarburizing methods, including gas, vacuum and iron ferritic nitrocarburizing, have been applied to production practice by engineers. Gas nitrocarburizing is performed at about 570 °C, just below the austenite range in the iron-nitrogen phase diagram. The treatment time is generally ranges from 1 to 3 hours [4, 7]. Ion (plasma) nitrocarburizing is a modified ion (plasma) nitriding method in which glow discharge technology is used to introduce nascent nitrogen to the surface of the material [8]. It is usually carried out at 570 °C to form a compound layer greater than 5µm and a surface hardness higher than 350 HV [4]. Vacuum nitrocarburizing is a subatmospheric pressure nitrocarburizing process using a basic atmosphere of 50% ammonia / 50% methane, as well as controlled oxygen additions of up to 2% [9].

The present paper deals with the case hardening results obtained by carbonitriding and various ferritic nitrocarburizing (gas, vacuum and ion) processes, paying particular attention to: (1) the microstructure and phase analysis of the carbonitrided and nitrocarburized specimens; (2) the changes in size (OD, ID, gap) and shape (flatness) of the piston and C-ring samples under carbonitriding and different nitrocarburizing conditions; (3) residual stresses at the surface of the samples.

### Materials and Experimental Procedures

The Navy C-ring specimens with dimensions of 50.8 mm OD × 31.75 mm ID, 6.35 mm gap width and 19.05 mm thickness were used, and ±0.127 mm dimensional tolerance was specified. The prototype stamped part was a torque converter piston, an important component of the transmission, with OD of 260 mm, thickness of 2.8 mm and a weight of 1.8 kg [10]. The C-rings and pistons were made from SAE 1010 plain carbon steel, the chemical composition of which is given in Table 1.

Table 1 Composition of SAE 1010 plain carbon steel [wt. %]

Material	C	Mn	P	S	Si	Cr	Ni	Mo	Cu	Al	V	Ti	B	Ca
SAE 1010 steel	0.12	0.43	0.008	0.008	0.03	0.03	0.01	0.01	0.02	0.052	0.001	0.002	0.0003	0.0001

Different temperature-time combinations of ferritic nitrocarburizing were applied to both the pistons and the C-ring samples to make a comparison with carbonitriding, as shown in Table 2. The heat treatment process schedule was identified using the symbols *a* to *e*.

Table 2 Heat treatment processing matrix for pistons and C-ring specimens

No.	Process	Heat Treatment Schedule	Symbol	Number of Samples	
				Pistons	C-rings
1	Ion ferritic nitrocarburizing	525 °C / 24 hrs+ nitrogen cooling	<i>a</i>	10	2
2	Gas ferritic nitrocarburizing (N potential)	525 °C / 52 hrs+ nitrogen cooling	<i>b</i>	10	2
3	Vacuum ferritic nitrocarburizing	580 °C / 10 hrs	<i>c</i>	10	2
4	Gas ferritic nitrocarburizing	580 °C / 2 hrs + water-base quenching	<i>d</i>	10	2
5	Gas carbonitriding	850 °C / 4 hrs + 100 °C oil quenching	<i>e</i>	5	1

Five piston samples were analyzed using X-ray Diffraction (XRD) techniques to determine the residual stress, according to the ASTM Standard E915 [11]. The (302) reflection of the  $\epsilon$ -phase ( $\text{Fe}_3\text{N}$ ) and the (211) martensite reflection were used to determine the residual stresses in the nitrocarburized and carbonitrided samples, respectively. The Cr target power was 40 kV and 40 mA, with a wavelength of 0.2291 nm. For the nitrocarburized samples, the Bragg angle ( $2\theta$ ) was set at 165.00° and the  $\Psi$  angles used were 0°, ±30.00°, ±23.46°, ±11.95° and ±7.58°. For the carbonitrided sample, the Bragg angle was 156.00°. The following  $\Psi$  angles were used: 0°, ±5.51°, ±12.00°, ±19.41°, ±25.00°. A detailed description of the XRD residual stress analysis method is given in references [12-14].

## Results and Discussion

**Optical Metallography.** The microstructures of the carbonitrided and nitrocarburized pistons are shown in Figures 1-2.

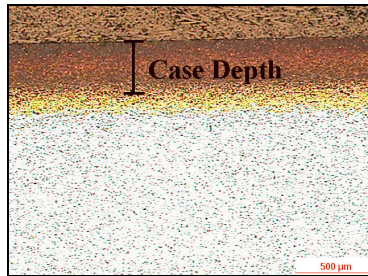


Fig. 1 Case depth of the carbonitrided piston

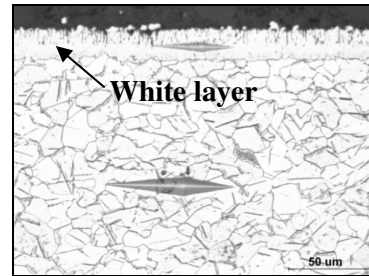


Fig. 2 Microstructure of the nitrocarburized piston

The average case depth of the carbonitrided piston is 0.321 mm in Figure 1. As shown in Figure 2, a very thin but well-formed white layer formed on the surface of nitrocarburized piston, accompanied by the penetration of a needle-like  $\gamma'$  phase into the diffusion zone. Microhardness indentations in the white layer and the diffusion zone were made using Tukon 2100B hardness tester under a load of 100 gram. The Knoop hardness of the white layer and the diffusion zone were HRC 62 and HRB 25.9, respectively.

**X-ray Phase Analysis.** The results of phase analysis of the nitrocarburized C-rings subjected to processes *a-d* are given in Tables 3.

Table 3 Phase analysis at the surface of the nitrocarburized C-ring samples

Process	Phases Analysis		
	Fe <sub>3</sub> C	Fe <sub>3</sub> N	Fe <sub>4</sub> N
<i>a</i>	+	+	+
<i>b</i>	-	+	+
<i>c</i>	-	+	-
<i>d</i>	-	+	-

In processes *a* and *b*, the compound layer consisted of  $\epsilon$ -phase and  $\gamma'$  phase, which is in agreement with the findings of Bell et al [8]. For all the nitrocarburized samples, Fe<sub>3</sub>N was detected at the surface. Fe<sub>3</sub>C was only detected in the sample from process *a*. The exact composition of the compound layer depends on the nitride-forming elements in the steel and the constituents of the heat treatment atmosphere [4].

**Comparison of Dimensional Distortion.** Four specified dimensions for each piston and C-ring sample both before and after nitrocarburizing and carbonitriding were measured using a Coordinate Measuring Machine (CMM). The average values obtained from the individual tests are reported as percentage dimensional changes in Tables 4 and 5.

Table 4 Dimensional changes of pistons [%]

Process	ID@-11mm	ID@-15mm	Total Flatness	Flatness Taper
<i>a</i>	0.0745	0.0913	16.27	23.69
<i>b</i>	0.0705	0.0915	5.11	21.94
<i>c</i>	0.0442	0.0694	49.27	99.73
<i>d</i>	0.0426	0.0664	39.67	76.47
<i>e</i>	-0.0615	-0.0055	515.30	507.84

The ID dimensions of pistons were evaluated at -11 mm and -15 mm longitudinal height positions from the lockup surface. Ferritic nitrocarburizing led to a small ID expansion, whereas an ID contraction was associated with carbonitriding.

The flatness is specified as the difference between the maximum and minimum values derived from a reference surface. The total flatness of a piston was evaluated at the lockup surface along six separate diameters (225, 230, 235, 240, 245, 250 mm). The flatness taper of a piston was scanned along the  $\pm X$  and  $\pm Y$  directions of the lockup surface. As shown in Table 4, the gas carbonitriding process resulted in severe flatness changes, which are more than 5 times larger than those for ferritic nitrocarburizing. Comparisons of dimensional changes between the different ferritic nitrocarburizing processes (*a*, *b*, *c* and *d*) are shown in Figures 3-6.

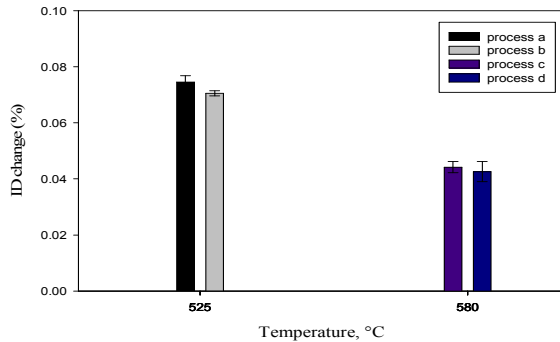


Fig. 3 ID change (@-11mm) of pistons as a function of nitrocarburizing temperature

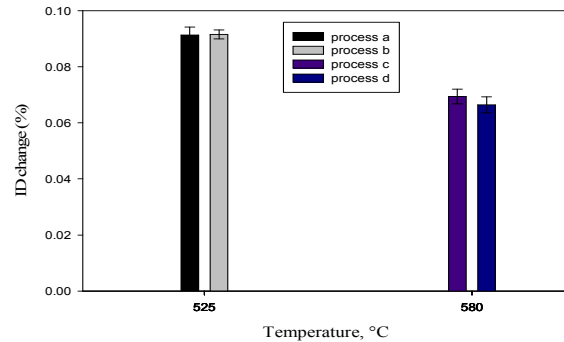


Fig. 4 ID change (@-15mm) of pistons as a function of nitrocarburizing temperature

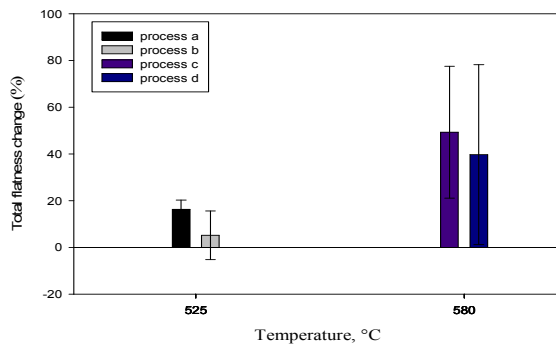


Fig. 5 Total flatness change of pistons as a function of nitrocarburizing temperature

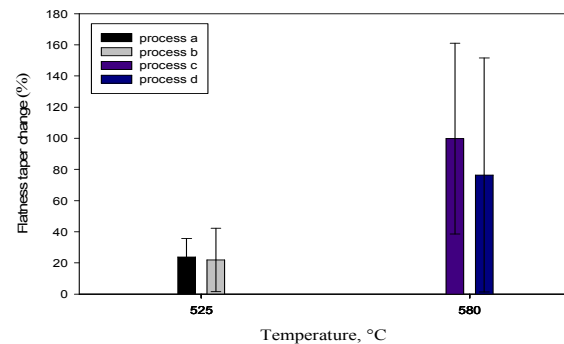


Fig. 6 Flatness taper change of pistons as a function of nitrocarburizing temperature

The ID changes resulting from different nitrocarburizing processes were similar at the same temperature and measuring position, see Figures 3 and 4. The process of ion nitrocarburizing (*a*) together with the gas nitrocarburizing and nitrogen cooling (*b*) produced larger ID changes but smaller flatness changes than the other processes. For the piston samples produced using the same nitrocarburizing process, the ID changes at -15 mm longitudinal height were always larger than those at -11 mm. The values of total flatness and flatness taper varied with the different nitrocarburizing processes, as shown in Figures 5 and 6. Vacuum nitrocarburizing (process *c*) led to the largest total flatness and flatness taper changes of the nitrocarburizing processes.

Table 5 Dimensional changes of C-ring samples [%]

Process	OD	ID	Gap	Flatness
<i>a</i>	0.0566	0.0466	0.0993	11.4596
<i>b</i>	0.0503	0.0202	-0.3416	3.4295
<i>c</i>	0.0464	0.0171	-0.0727	-4.2994
<i>d</i>	0.0511	0.0241	0.0441	10.3882
<i>e</i>	0.1146	0.1565	2.4424	-8.0508

Table 5 shows that both the nitrocarburizing and carbonitriding led to OD and ID expansions of the C-ring samples. Carbonitriding resulted in the largest OD, ID and gap changes. The flatness value was determined by scanning approximately 2100 points along the perimeter of a C-ring sample. The C-ring samples experienced smaller flatness distortion after carbonitriding than the thinner piston samples. Comparisons between the different ferritic nitrocarburizing processes (*a*, *b*, *c* and *d*) are shown in Figures 7-10.

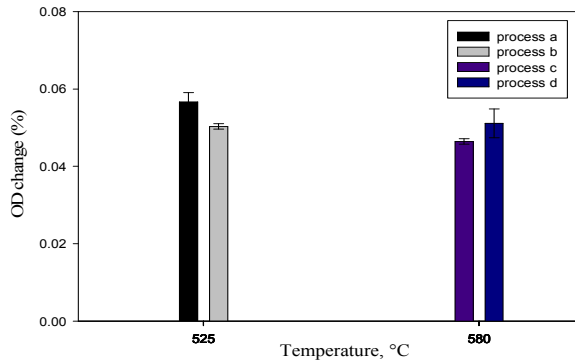


Fig. 7 OD change of C-rings as a function of nitrocarburizing temperature

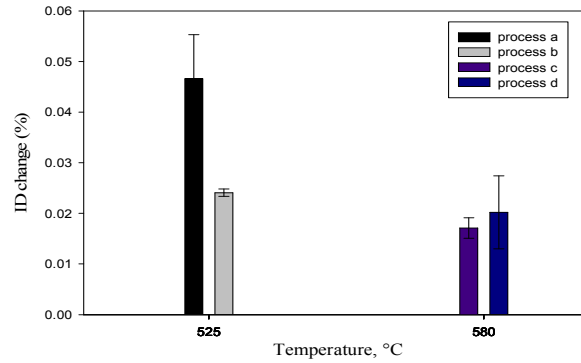


Fig. 8 ID change of C-rings as a function of nitrocarburizing temperature

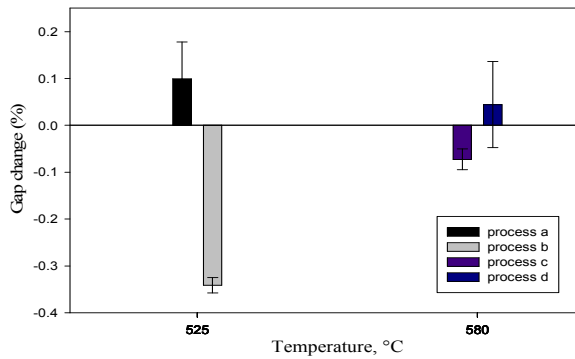


Fig. 9 Gap change of C-rings as a function of nitrocarburizing temperature

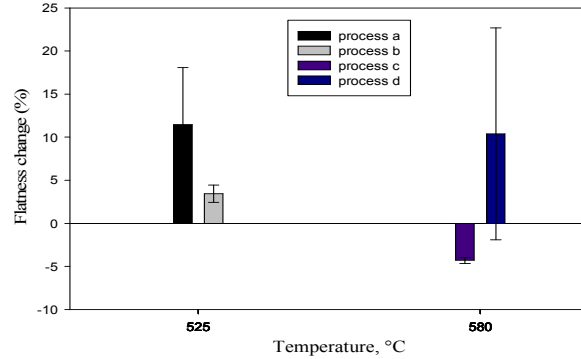


Fig. 10 Flatness change of C-rings as a function of nitrocarburizing temperature

As shown in Figures 7 and 8, ion nitrocarburizing (*a*) produced the largest OD and ID changes. Gas nitrocarburizing and quenching (*d*) resulted in larger OD and ID changes than vacuum nitrocarburizing (*c*) at the same temperature. The gap tended to close up after gas nitrocarburizing and nitrogen cooling (*b*) and vacuum nitrocarburizing (*c*) in Figure 9. The values of flatness were increased after nitrocarburizing except for the vacuum nitrocarburized C-rings, see Figure 10.

**Residual Stress Measurements.** The results of the residual stress measurements of the pistons are given in Table 6. Ferritic nitrocarburizing resulted in tensile residual stresses in the  $\epsilon$ -nitride surface layer, which is in agreement with the findings of Kolozsváry [15] and Watkins et al [16]. In comparison, carbonitriding led to favorable compressive residual stresses, which can improve the surface fatigue resistance of the specimen [17,18].

Table 6 Residual Stress Analysis of Pistons

Sample No.	Normal Stress [MPa]	Process
Piston N 1	224.1 ± 18.6	<i>a</i>
Piston N 2	172.4 ± 9.7	<i>b</i>
Piston N 3	262.7 ± 20.0	<i>c</i>
Piston N 4	252.3 ± 19.3	<i>d</i>
Piston N 5	-188.9 ± 26.2	<i>e</i>

## Conclusions

1. Both the gas carbonitriding and ferritic nitrocarburizing resulted in size and shape distortions in the pistons and Navy C-ring specimens. The gas carbonitriding led to severe flatness changes in the pistons and larger OD, ID and gap changes in the C-ring samples than gas, vacuum or ion ferritic nitrocarburizing.
2. A comparison between the different ferritic nitrocarburizing processes (*a*, *b*, *c* and *d*) shows that: The ion nitrocarburizing (*a*) and gas nitrocarburizing and nitrogen cooling (*b*) produced larger size (OD, ID and gap) changes but smaller shape (flatness) changes in pistons and C-ring specimens than the vacuum nitrocarburizing (*c*) and gas nitrocarburizing and quenching (*d*).
3. Nitrocarburizing resulted in tensile residual stresses in the  $\epsilon$ -nitride surface layer of the pistons, whereas compressive residual stresses were present at the surface of the carbonitrided samples.

## References

- [1] J. R. Davis, in Surface Hardening of Steels: Understanding the Basics, edited by J. R. Davis, chapter, 5, ASM International (2002).
- [2] G. Krauss: Steels: Processing, Structure, and Performance, ASM International (2005).
- [3] J. Dossett, in: Carbonitriding, volume 4 of ASM Handbook, Heat Treating, ASM International (1991).
- [4] J. R. Davis, in Surface Hardening of Steels: Understanding the Basics, edited by J.R. Davis, chapter, 7, ASM International (2002).
- [5] D. Pye: Practical nitriding and ferritic nitrocarburizing, ASM International (2003).
- [6] A. Wells: Mater. Sci., Vol. 20 (1985), p. 2439-2445.
- [7] T. Bell, in: Gaseous and Plasma Nitrocarburizing, volume 4 of ASM Handbook, Heat Treating, ASM International (1991).
- [8] T. Bell, Y. Sun and A. Suhadi: Vacuum, Vol. 59 (2000), p. 14-23.
- [9] Information on [http://www.tdcoating.com/td\\_glossary\\_terms9a.htm#v.html](http://www.tdcoating.com/td_glossary_terms9a.htm#v.html).
- [10] P. Schobesberger, T. Streng and S. Abbas: Industrial Heating, Vol. 69 (2) (2002), p. 30-34.
- [11] Standard Test Method for Verifying the Alignment of X-Ray Diffraction Instrumentation for Residual Stress Measurement, E915-96, ASTM International (2002).
- [12] J. A. Pineault, M. Belassel and M. E. Brauss, in: X-Ray Diffraction Residual Stress Measurement in Failure Analysis, volume 11 of ASM Handbook, Failure Analysis and Prevention, ASM International (2002).
- [13] C. Ruud, in: Measurement of Residual Stresses, edited by G. Totten, M. Howes and T. Inoue, Handbook of Residual Stress and Deformation of Steel, ASM International (2002).
- [14] H. W. Walton, in: Deflection Methods to Estimate Residual Stress, edited by G. Totten, M. Howes and T. Inoue, Handbook of Residual Stress and Deformation of Steel, ASM International (2002).
- [15] Z. Kolozsváry, in: Residual Stress in Nitriding, edited by G. Totten, M. Howes and T. Inoue, Handbook of Residual Stress and Deformation of Steel, ASM International (2002).
- [16] T. R. Watkins, R. D. England, C. Klepser and N. Jayaraman: Advances in X-ray Analysis, Vol. 43 (2000), p. 31-38.
- [17] T. Réti, in: Residual Stresses in Carburized, Carbonitrided, and Case-Hardened Components, edited by G. Totten, M. Howes and T. Inoue, Handbook of Residual Stress and Deformation of Steel, ASM International (2002).
- [18] C. Kanchanomai and W. Limtrakarn: Materials Engineering and Performance, Vol. 17 (6) (2008), p. 879-887.

## **THERMEC 2009**

10.4028/www.scientific.net/MSF.638-642

### **Study on the Dimensional Changes and Residual Stresses in Carbonitrided and Ferritic Nitrocarburized SAE 1010 Plain Carbon Steel**

10.4028/www.scientific.net/MSF.638-642.829

## **DOI References**

[5] D. Pye: Practical nitriding and ferritic nitrocarburizing, ASM International (2003).

10.2466/PMS.96.2.549-577

[6] A. Wells: Mater. Sci., Vol. 20 (1985), p. 2439-2445.

10.1007/BF00556072

[10] P. Schobesberger, T. Streng and S. Abbas: Industrial Heating, Vol. 69 (2) (2002), p. 30-34.

10.1053/tvj.2001.0608

[18] C. Kanchanomai and W. Limtrakarn: Materials Engineering and Performance, Vol. 17 (6) (2008), p. 879-887.

10.1007/s11665-008-9212-x